

Crack Paths in Unidirectional Fibre-Reinforced Brittle-Matrix Materials through Two Computational Models

Roberto Brighenti, Andrea Carpinteri, Andrea Spagnoli and Daniela Scorza

Department of Civil–Environmental Engineering and Architecture, University of Parma, Viale Usberti 181/A, 43124 Parma, Italy; E-mail: brigh@unipr.it

ABSTRACT. *In the present paper, both a continuum FE approach and a lattice-based micromechanical approach are employed to analyse fibre-reinforced brittle-matrix materials by adopting a cohesive-like fracture behaviour, properly modified taking into account the fibre bridging effect. The basic assumptions and theoretical background of such two computational approaches are outlined, and some benchmark analyses related to random and unidirectional fibre-reinforced brittle-matrix structural components under monotonic tensile loading are discussed.*

INTRODUCTION

As is well-known, brittle or quasi-brittle materials suffer from several drawbacks (such as low tensile strength, low fracture and fatigue resistance, poor wear resistance) which can be reduced by adding fibres to the matrix material. Reinforcing fibres improve fracture toughness, ductility, durability, fatigue resistance of brittle-matrix materials. Nevertheless, fracture can take place even if fibres produce a shield effect in the crack formation and propagation, such an effect being due to the bridging stresses developed across the crack faces [1, 2]. The composite is macroscopically isotropic when fibres are randomly distributed, while the composite behaves macroscopically as an anisotropic material if the arrangement of fibres in the matrix follows a preferential orientation (unidirectional material) [3, 4]. In the latter case, the crack propagation is heavily affected by such a macroscopic mechanical behaviour; further, the principal stresses due to the remote applied load and the bridging stresses might act along different skewed directions with respect to the crack orientation, and the crack grows under mixed mode condition.

Since FRC materials are multiphase, they present some phenomena such as matrix cracking, crack bridging effects due to fibres, fibre debonding and fibre breaking which must be correctly modelled. In order to examine such materials, various approaches can be used, such as micromechanical models [2, 5, 6] and homogenization models [7, 8]. Due to low fracture toughness of brittle materials, crack propagation up to failure can easily occur even if the fibre phase has a beneficial crack bridging effect limiting such a phenomenon. Several models can be found in the literature: classical smeared crack approaches [9], models based on the description of the evolving crack geometry [10], finite element enrichment approaches [11], interface element approaches [12], meshless methods [13], discontinuous formulations [14], and so on. Discrete models, such as the well-known lattice model [15], can also be employed.

In the present paper, following a recent work by the present authors [16], two different mechanical models are compared: (i) a continuum model based both on a fracture energy approach for the brittle matrix [5] and on a micromechanical approach to examine the macroscopic reinforcing effects due to fibres [17]; (ii) a micromechanical discrete lattice model [6] that can be used to simulate heterogeneous materials and multi-phase composites such as fibre-reinforced ones. The basic assumptions and theoretical background of such approaches – especially related to the case of unidirectional reinforced materials – are briefly discussed. Then, some experimental data related to both random and unidirectional fibre-reinforced cementitious composites under monotonic tensile loading are analysed.

FRACTURE SIMULATION IN BRITTLE OR QUASI-BRITTLE MATERIALS

A Continuum Approach to Fracture

A crack process zone in a continuum material can mathematically be represented as a high strain localisation occurring in a very narrow region. Assuming the existence of a discontinuity of the displacements in a solid, the discontinuous displacement field can be expressed as the sum of its continuous part and discontinuous part [14]. The mechanical behaviour of a cracked body can conveniently be described by a cohesive-friction law for the cracked zone and by an elastic or an elastic-plastic law for the uncracked (bulk) region. According to the cohesive crack model [1], the normal, $\sigma_c(u_c)$, and tangential stress, $\tau_c(u_c, v_c)$, transmitted across the crack faces, can be written as follows:

$$\sigma_c(u_c) = f_t \cdot e^{\frac{2f_t(u_0 - u_c)}{2G_f - f_t \cdot u_0}} \quad \text{with} \quad \sigma_c(u_c) \xrightarrow[u_c \rightarrow \infty]{} 0^+ \quad (1)$$

$$\tau_c(u_c, v_c) = \begin{cases} \text{sign}(v_c) \cdot [\sigma_c(u_c) \cdot \beta] \cdot \left[1 - \left(\frac{u_c}{2 \cdot r_c} \right)^m \right] & \text{if } 0 < u_c < 2 \cdot r_c \quad \text{and} \quad v_c \neq 0 \\ 0 & \text{if } u_c > 2 \cdot r_c \quad \text{or} \quad v_c = 0 \end{cases} \quad (2)$$

where f_t is the maximum tensile strength of the material, u_0 is the lower crack opening limit at which the bridging process starts, G_f is the fracture energy of the material (energy for unit surface crack), r_c is the mean asperity size of the crack surface roughness, β is a friction coefficient, m is an experimentally determined parameter, u_c and v_c are the relative crack displacements measured normally and tangentially to the crack surface, respectively.

The FE formulation of the above problem can use an appropriate stress field correction in the cracked element, in order to get the unbalanced nodal force vector $\mathbf{f}_{e,u}^{(i)}$ at the generic iteration step i :

$$\mathbf{f}_{e,u}^{(i)} = \mathbf{f}_{e,ext}^{(i)} - \int_{\Omega_e} \mathbf{B}^t \cdot \boldsymbol{\sigma}_{rel}(\mathbf{w}_c) d\Omega \quad (3)$$

which must be iteratively driven to very small values. In Eq. (3), $\boldsymbol{\sigma}_{rel}(\mathbf{w}_c)$ is the stress tensor fulfilling some stress relaxation requirements according to Eq. (2), \mathbf{B} is the generic compatibility matrix of the finite element, and $\mathbf{f}_{e,ext}^{(i)}$ is the external nodal force vector at the iteration step i .

A Lattice Approach to Fracture

The domain occupied by the material is discretized by a triangular lattice (in order to reduce the bias of the crack trajectory, the triangular lattice can be made irregular by randomly perturbing the nodal coordinates), having hexagonal unit cells with truss elements of length l . The main advantage of the lattice models is to replace the tensorial quantities (related to the continuum occupied by the material) with vectorial quantities.

The Young modulus of the truss elements in the lattice model determines the stiffness of the material. The relationship between the Young modulus of the truss (\bar{E}) and that of the material (E), evaluated by equating the elastic strain energy of the material occupying an hexagonal unit cell with that of the lattice occupying the same region [15], is $\bar{E} = (\sqrt{3}lE)/(2A)$, where A is the cross-sectional area of the truss. From now onwards we adopt the following notation: a bar above the symbol means that the quantity is related to truss elements of the lattice model, whereas the plain symbol means that the quantity is related to the material.

Then, the components $\sigma_x, \sigma_y, \tau_{xy}$ of a plane stress field with respect to the x-y coordinate system are connected to the axial stresses acting in the trusses through the following relationship [6]:

$$\begin{Bmatrix} \bar{\sigma}^{(1)} \\ \bar{\sigma}^{(2)} \\ \bar{\sigma}^{(3)} \end{Bmatrix} = \frac{l}{A} \begin{bmatrix} \sqrt{3}/2 & -\sqrt{3}/6 & 0 \\ 0 & \sqrt{3}/3 & 1/2 \\ 0 & \sqrt{3}/3 & -1/2 \end{bmatrix} \begin{Bmatrix} \sigma_x \\ \sigma_y \\ \tau_{xy} \end{Bmatrix} \quad (4)$$

where the superscript ((1), (2) or (3)) identifies the truss orientation with respect to the x-y frame (the direction cosines of the truss elements are $n_x^{(1)} = 1, n_y^{(1)} = 0$; $n_x^{(2)} = 1/2, n_y^{(2)} = \sqrt{3}/2$; $n_x^{(3)} = -1/2, n_y^{(3)} = \sqrt{3}/2$).

The tensile behaviour of a quasi-brittle material is described according to the cohesive crack approach. Hence, the stress-strain curve is the result of the contribution of two constitutive laws: that of the bulk material, here assumed to be linear with Young modulus in tension equal to that in compression, and the crack bridging law of the cracked material. The resulting stress-strain curve is characterized by a perfectly-elastic behaviour in compression; the tensile behaviour is elastic up to the first cracking stress, and then a linear postcracking curve with a softening branch follows.

Now let us note that, having Eq. (4) in mind and examining a uniaxial stress condition, the first cracking stress \bar{f}_t of the truss is equal to $(l\sqrt{3}/(2A))f_t$, where f_t is the first cracking stress of the material.

In line with the cohesive crack approach, the area under the stress σ against crack opening w curve (characterized by a first cracking stress f_t and an ultimate crack

opening w_u) is equal to the Mode I fracture energy G_f (hence, for a linear curve σ against w , $w_u = 2G_f/f_t$). This concept can be translated to the truss elements of the lattice model, if one assumes to smear the crack opening along the length of the truss. The ultimate cracking strain $\bar{\varepsilon}_u$ turns out to be $\bar{\varepsilon}_u = (4G_f)/(3l f_t)$ [6].

MECHANICS OF FIBRE-REINFORCED MATERIALS

In this Section, the modelling of the reinforcing effects (due to fibres) within the framework of the two theoretical approaches being compared is described. Unless otherwise specified, details of such a modelling can be found in Refs [5, 17] and Refs [2, 6] for the continuum model and the lattice model, respectively.

Mesomechanical Model in the Continuum Approach

The heterogeneous (composite) material is supposed to consist of a matrix phase (denoted by the subscript m) and a fibre phase (denoted by the subscript f) embedded in the matrix (Fig. 1). The composite material (having characteristic size D) is assumed to have macroscopically the same mechanical characteristics of a small Representative Volume Element (RVE, having characteristic size $d \ll D$).

The tangent elastic tensor of the macroscopically homogeneous composite can be determined through an energy balance between the composite and the equivalent macroscopically homogeneous material:

$$\mathbf{C}'_{eq} = \mu \cdot \mathbf{C}'_m + \eta_f \cdot E_f \cdot \underbrace{\left[s(\varepsilon_f^m) + \varepsilon_f^m \cdot \frac{ds(\varepsilon_f^m)}{d\varepsilon_f^m} \right]}_{\mathbf{C}'_f} \cdot \int_0^\pi \int_0^\pi p_\varphi(\varphi) \cdot p_\theta(\theta) \cdot (\mathbf{F} \otimes \mathbf{F}) d\varphi d\theta \quad (5)$$

where $\mathbf{C}'_m, \mathbf{C}'_f, \mathbf{C}'_{eq}$ are the tangent elastic tensors (of the matrix, of the fibres and of the equivalent material, respectively); E_f is the Young modulus of the fibre phase; $\mathbf{F} = \mathbf{k} \otimes \mathbf{k}$ is a second-order tensor, where \mathbf{k} is the unit vector parallel to the fibre axis, $\mathbf{k} = \{\sin\theta \cdot \cos\varphi \quad \sin\theta \cdot \sin\varphi \quad \cos\theta\}$ (Fig. 1). In Eq.(5), ε_f^m is the strain (in the matrix)

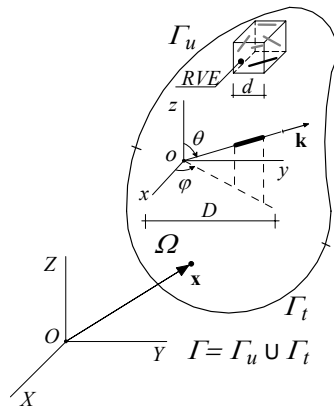


Figure 1. Scheme of the RVE and identification of the fibre orientation in the 3D space.

measured in the fibre direction, σ_f is the actual fibre stress. Furthermore, $\mu_m = V_m / V$, $\eta_f = V_f / V$ represent the matrix volume fraction and fibre volume fraction in the composite RVE, respectively. Finally, $s(\varepsilon_f^m)$ is the sliding scalar function that quantifies the matrix-fibre strain jump, $[[\varepsilon_{f-m}]] = \varepsilon_f^m \cdot [1 - s(\varepsilon_f^m)]$, occurring in the case of matrix-fibre debonding. Preferential orientation of the fibres in one particular space direction can be taken into account through suitable probability distribution density functions $p_\varphi(\varphi)$, $p_\theta(\theta)$ of the orientation angles φ, θ :

$$p_\alpha(\alpha) = A_\alpha(\alpha) + B_\alpha(\alpha) + C_\alpha(\alpha) \quad \text{with} \quad A_\alpha(\alpha) = \frac{1}{\sqrt{2 \cdot \pi \cdot \delta_\alpha^2}} \cdot e^{-\frac{1}{2} \left(\frac{\alpha - \mu}{\delta_\alpha} \right)^2},$$

$$B_\alpha(\alpha) = \frac{1}{\sqrt{2 \cdot \pi \cdot \delta_\alpha^2}} \cdot e^{-\frac{1}{2} \left(\frac{\alpha - \pi - \mu}{\delta_\alpha} \right)^2}, \quad C_\alpha(\alpha) = \frac{1}{\sqrt{2 \cdot \pi \cdot \delta_\alpha^2}} \cdot e^{-\frac{1}{2} \left(\frac{\alpha + \pi - \mu}{\delta_\alpha} \right)^2} \quad (6)$$

with $\alpha = \varphi, \theta$.

The above functions $p_\alpha(\alpha)$ with $\alpha = \varphi, \theta$, defined in the intervals $0 \leq \alpha \leq \pi$, are theoretically formulated by assuming a Gaussian-like expression, which attains the maximum value at $\alpha = \bar{\varphi}, \bar{\theta}$ (mean values of the Euler angles), and the minimum value at $\alpha = \bar{\varphi} \pm \pi/2, \bar{\theta} \pm \pi/2$. Further, the cumulated probability over the function domain is equal to one. The parameter μ represents the mean value of the probability distribution density functions (i.e. $\mu = \bar{\varphi}$ or $\mu = \bar{\theta}$), whereas δ_φ and δ_θ are the corresponding variances. The case of randomly oriented fibres can be obtained by setting $p_\varphi(\varphi) = 1/2\pi$ and $p_\theta(\theta) = \sin(\theta)$.

In order to take into account the fibre-matrix debonding, we introduce the sliding function $s(\varepsilon_f^m)$ that allows us to write the fibre strain ε_f as a function of the matrix strain ε_f^m , that is, $\varepsilon_f = s(\varepsilon_f^m) \cdot [(\mathbf{k} \otimes \mathbf{k}) : \varepsilon]$ [17]. the fibre-matrix debonding can be taken into account properly multiplying the integral in Eq. (5) by a function depending on such a relative fibre-matrix sliding.

Note that the maximum tensile stress along a fibre is always reached at its centre [17]. When such a maximum stress reaches the fibre tensile strength, i.e. $\sigma_f(0) \geq f_{t,f}$, the fibre is assumed to break in two parts having the same length.

Fibre Crack Bridging in the Lattice Approach

The tensile behaviour of a fibre-reinforced composite material is described according to the cohesive crack approach. Hence, the stress-strain curve for the above cracked matrix is combined with the crack bridging law due to fibres. The resulting stress-strain curve is characterized by a perfectly-elastic behaviour in compression; the tensile behaviour is elastic up to the first cracking stress, and then a linear piecewise postcracking curve with softening branches follows.

Assuming a uniform distribution for the fibres, the peak stress due to the fibre crack bridging is [2]:

$$\sigma_0 = \frac{\eta_f 2L_f \tau_0}{D_f} \left(\frac{1 + f e^{f\pi/2}}{1 + f^2} \right) \quad (7)$$

where f = snubbing coefficient (usually ranging from 0.7 to 0.9), τ_0 = frictional bond stress, D_f = fibre diameter, $2L_f$ = fibre length, η_f = volume fraction of fibres.

If unidirectional fibres are examined, σ_0 depends on the angle $\hat{\alpha}$ between the fibre direction and the truss direction in the lattice:

$$\sigma_0 = \frac{\eta_f 2L_f \tau_0}{D_f} e^{f\hat{\alpha}} \quad (8)$$

The peak stress due to the fibre crack bridging in the truss of the lattice normal to a putative Mode I crack plane is equal to $\bar{\sigma}_0 = (l\sqrt{3}/(2A))\sigma_0$ (e.g. see, in Eq. 4, the stress in the truss (1) when x is the loading axis).

The characteristic cracking strain values of the crack bridging curve due to fibres can be determined by smearing the crack opening along the length of the truss, namely: $\bar{\varepsilon}_0 = w_0/l$, $\bar{\varepsilon}_{u,f} = w_{u,f}/l$, where $w_0 = (L_f^2 \tau_0) / [(1 + \rho)E_f D_f]$ (with $\rho = (E_f \eta_f) / [E(1 - \eta_f)]$) is the crack opening at the peak stress of the crack bridging law due to fibres, and $w_{u,f} = L_f$ is the ultimate crack opening of the bridging law due to fibres.

COMPARISON BETWEEN NUMERICAL AND EXPERIMENTAL RESULTS

The fracture behaviour of plain and fibre-reinforced concrete coupons under tensile loading is examined herein by means of the two computational models being compared. The first one, based on a continuum approach, has been implemented in an in-house code, whilst the second one, based on a lattice approach, has been implemented in the subroutine UMAT of the commercial FE code ABAQUS.

An experimental campaign related to prismatic Reactive Powder Concrete (RPC) specimens subjected to tensile stress is examined [18]. The specimens have a total length equal to 700 mm and cross section of 50x20 mm (Fig. 2). The mechanical parameters of the RPC concrete are the following: Young modulus $E = 50$ GPa, ultimate tensile strength $f_t = 8.0$ MPa, fracture energy $G_f = 30$ N/m [19]. The relevant parameters for unidirectional steel fibres are: fibre volume $\eta_f = 2.0\%$, Young modulus $E_f = 210$ GPa, fibre length $2L_f = 13$ mm and diameter $D_f = 0.16$ mm, while the limit matrix-fibre shear stress is equal to $\tau_0 = 2.0$ MPa. The analysis is performed under displacement control by imposing a progressive upward vertical displacement at the top of the specimens. A plane stress condition is assumed. Five orientations of fibres are considered ($\varphi = 0^\circ, 30^\circ, 45^\circ, 60^\circ, 90^\circ$) together with the cases of random fibres and of plain concrete (no fibres).

In Fig. 2, some crack paths of the continuum and the lattice models are shown.

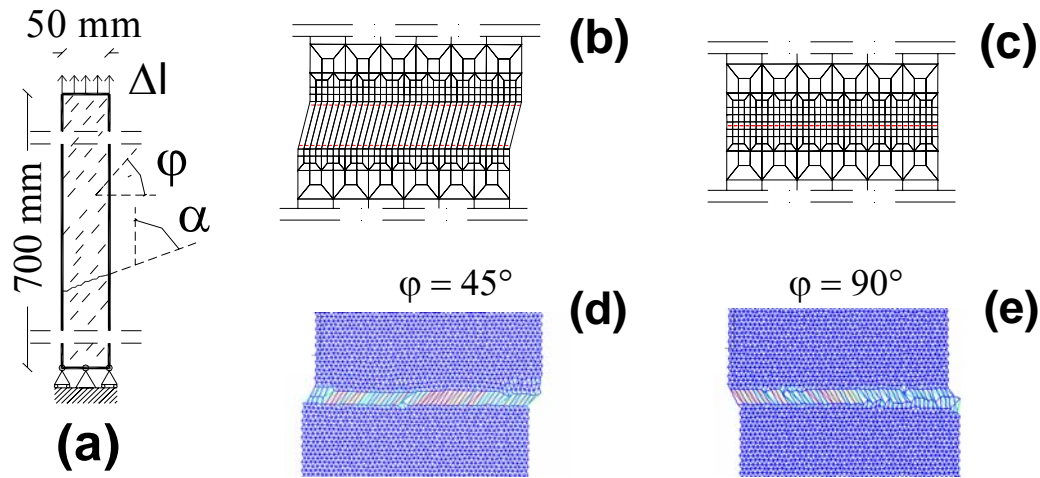


Figure 2. (a) Geometry of the specimen [18]; (b, c) crack path for the continuum model for fibre orientation of 45° and 90°; (d, e) crack path for the lattice model for fibre orientation of 45° and 90°.

Vertical load against top vertical displacement curves are reported in Figure 3a-b. The curves have the same slope in the elastic branch both for the continuum model and for the lattice one, while the peak load is slightly different, up to 20%. Further, another difference between the two models is the residual strength in the post-peak stage. In Figure 4, the crack orientation α against the fibre orientation φ , obtained through the continuum model and the lattice model, are compared with the orientation observed experimentally [18]. The continuum model shows an evident dependence of the initial crack orientation on the fibre orientation, while such a dependence is negligible for the lattice model.

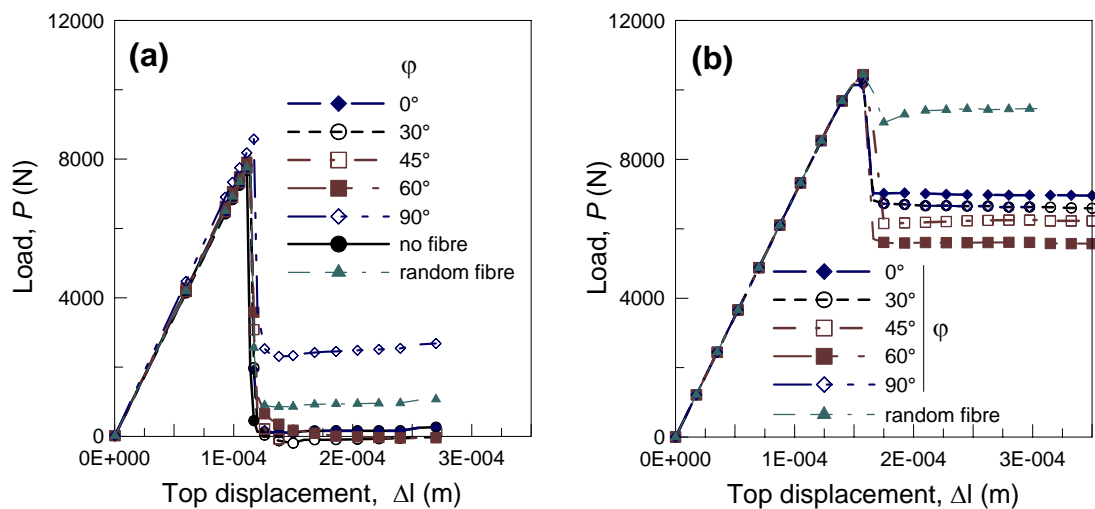


Figure 3. Vertical load against top displacement according to (a) the continuum FE model and (b) the lattice model.

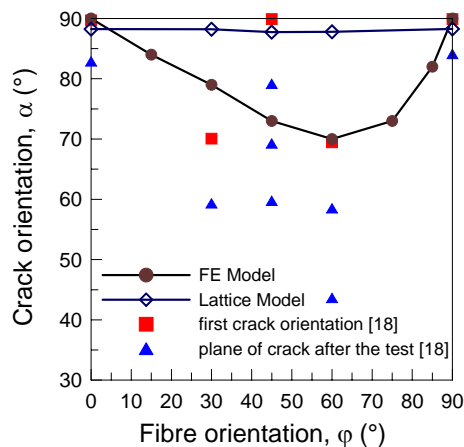


Figure 4. Crack orientation against fibre orientation according to experiments, the continuum FE model and the lattice model.

CONCLUSIONS

In the present paper, the crack formation and propagation in random and unidirectional fibre-reinforced quasi-brittle materials have been analysed by using a continuum FE model and a microstructural lattice model. The main theoretical aspects to describe the matrix fracture and the fibre bridging effects have been outlined, and experimental results related to fibre-reinforced concrete specimens under tensile loading have been examined.

REFERENCES

- Hillerborg, A., Modéer, M., Peterson, P.E. (1976) *Cement Concrete Res.*; **6**, 773–782.
- Carpinteri, A., Spagnoli, A., Vantadori, S. (2006) *Int. J. Solids Struct.*; **43**, 4917–4936.
- Kalamkarov, A.L., Kolpakov, A.G. (1996) *Compos. Part B-Eng.*; **27B**, 485–492.
- Ngolle, A., Pe´ra, J. (1997) *Adv. Cem. Based Mater.*; **6**, 130–137.
- Carpinteri, A., Brighenti, R. (2009) *Comp. Mater. Sci.*; **45**, 367–377.
- Spagnoli, A. (2009) *Comp. Mater. Sci.*; **46**, 7–14.
- Kalamkarov, A.L., Liu, H.Q. (1998) *Compos. Part B-Eng.*; **29B**, 643–653.
- Hori, M., Nemat-Nasser, S. (1999) *Mech. Mater.*; **31**, 667–682.
- Tin-Loi, F., Tseng, P. (2003) *Comput. Method Appl. M.*; **192**, 1377–1388.
- Bouchard, P.O., Bay, F., Chastel, Y., Toven, I. (2000) *Comput. Method Appl. M.*; **189**, 723–742.
- Jirásek, M., Belytschko, T. (2002) In: *Proceedings of WCCM V*; Vienna.
- Alfaiate, J., Pires, E.B., Martins, J.A.C. (1997) *Comput. Struct.*; **63**, 17–26.
- Belytschko, T., Lu, Y.Y., Gu, L. (1994) *Int. J. Numer. Meth. Eng.*; **37**, 229–256.
- Sancho, J.M., Planas, J., Cendón, D.A., Reyes, E., Gálvez, J.C. (2007) *Eng. Fract. Mech.*; **74**, 75–86.
- Schlangen, E., van Mier, J.G.M. (1992) *Mater. Struct.*; **25**, 534–542.
- Brighenti, R., Carpinteri, A., Spagnoli, A., Scorza, D. (2012) *Engng Fract Mech*s available online.
- Brighenti, R. (2004) *Comp. Mater. Sci.*; **29**, 475–493.
- Bayard, O. and Plé, O. (2003) *Eng. Fract. Mech.*; **70**, 839–851.
- Richard, P. Cherezy, M. (1995) *Annales ITBTP*, **532**, 85–102.